Oxidative Stress and Apoptosis are Markers in Renal Toxicity Following Egyptian Cobra (Naja haje) Envenomation

Article *in* Pakistan journal of zoology · November 2014

CITATIONS
0

READS
119

1 author:

Ahmed E Abdel Moneim
Helwan University
161 PUBLICATIONS **2,426** CITATIONS

SEE PROFILE

Pakistan J. Zool., vol. 46(6), pp. 1719-1730, 2014.

Oxidative Stress and Apoptosis are Markers in Renal Toxicity Following Egyptian Cobra (*Naja haje*) Envenomation

Mohamed A. Dkhil,[1,2] Saleh Al-Quraishy,[1] Abdel Razik H. Farrag,[3] Ahmed M. Aref,[4] Mohamed S. Othman[5] and Ahmed E. Abdel Moneim[2,*]

[1]*Department of Zoology, College of Science, King Saud University, Riyadh, Saudi Arabia.*
[2]*Department of Zoology and Entomology, Faculty of Science, Helwan University, Cairo, Egypt.*
[3]*Pathology Department, Medical Research Division, National Research Centre, Cairo, Egypt.*
[4]*Biological Science Department, Faculty of Dentistry, Modern Sciences and Arts University, Giza, Egypt.*
[5]*Biochemistry and Molecular Biology Department. Faculty of Biotechnology, Modern Science and Arts, Giza, Egypt.*

Abstract.- Snakebite is a serious and important problem in tropical and subtropical countries including Egypt. The venom of Egyptian cobra (*Naja haje*; L.) is complex, and it has been considered as a good source of short neurotoxins and several cytotoxins. In this study, oxidative stress inductions as well as apoptotic effects of the Egyptian cobra crude venom at a dose of 0.025mg/kg (intraperitoneal injection; *i.p.*) has been investigated in kidney of rats after 4 h. Twelve rats divided into 2 groups, Group I served as control group, Group II received *i.p.* injection of 0.025mg/kg of crude venom. The venom enhanced lipid peroxidation and nitric oxide productions in the kidney with concomitant reduction in glutathione content and superoxide dismutase, catalase, glutathione peroxidase, glutathione reductase and glutathione-S-transferase activities were inhibited. Moreover, the venom induced a renal injury as indicated by histopathological changes in the kidney tissue with an elevation in serum creatinine and urea. In addition, the renal ultrastructural changes were in the form of blebbing of visceral epithelial cells, and foot process disorganization. Also, the glomerular capillaries lined by hypertrophied endothelial cells. These findings were associated with the pro-apoptotic action in the kidney. The results suggest that Egyptian cobra venom stimulates oxidative stress to induce apoptosis in renal tissue through inhibition of mitochondrial respiration in male rats.

Keywords: Egyptian cobra venom, renal toxicity, oxidative stress, apoptosis.

INTRODUCTION

Snakebite envenomation is known to man since antiquity and many references to snakebite are found in the oldest medical writings. There are more than 2.5 million venomous snake bites annually, with greater than 125000 deaths. The risk is highest in the tropics and West Africa, predominantly among rural population (Gutierrez *et al*., 2006). Snake venoms are a mixture of complex toxins that may be independent, synergistic or antagonistic (Al-Quraishy *et al*., 2014). Broadly, there are two types of toxins namely neurotoxins, which attack the central nervous system and hemotoxins which target the circulatory system (Markland, 1998). It is important to understand that the actual mixture of toxins in the venom will vary by individual species and also by age and season (Al-Sadoon *et al.*, 2013).

The venom of Egyptian cobra (*Naja haje*) is complex, and it has been a good source of short neurotoxins and several cytotoxins. From this venom the purification and the primary structure of two short neurotoxins and of 14 cytotoxins have been reported. Besides the toxins, *N. haje* venom contains also low-molecular-weight polypeptides, usually of relative low toxicity and of completely distinct immunochemical properties (Joubert and Taljaard, 1978).

Although, nearly all snakes with medical relevance can induce nephropathy, leading to acute renal failure (ARF), it is unusual except with bites by Egyptian cobra. This action was attributed to the effect of different venom toxins, such as myotoxins, cytotoxins, phospholipases, and cardiotoxins (Rahmy, 2001). It was found that myotoxin probably causes renal damage due to myoglobin cast nephropathy. Venom phospholipase is known to be toxic to cells and believed to be responsible for disturbing the cell membrane permeability

* Corresponding author: aest1977@helwan.edu.eg
0030-9923/2014/0006-1719 $ 8.00/0

(Mukherjee and Maity, 1998). Phospholipase may also alter the mitochondrial respiratory functions and induce a hemolytic activity (Mukherjee *et al*., 1998). Cobra cytotoxins and cardiotoxins may also disturb different cell types (Rahmy, 2001). Cytotoxin lytic activity in synergy with various phospholipases of cobra venom was also reported (Chaim-Matyas *et al*., 1995).

Nevertheless, the oxidative stress induced by the venom of *N. haje* was not sufficiently covered in the available literature (El Hakim *et al*., 2011). Thus, it is so special interest to examine the possible effects of LD_{50} of the crude venom in kidney of rats after 4 h of envenomation.

MATERIALS AND METHODS

Experimental animals

Adult male Wistar albino rats weighing 120–150 g were obtained from the Holding Company for Biological Products and Vaccines (Vacsera, Cairo, Egypt). After an acclimatization period of one week, the animals were divided into two groups (6 rats per group) and housed in wire bottomed cages under standard conditions of illumination with a 12 h light-dark cycle at 25±1ºC. They were provided with water and a balanced diet *ad libitum*. We have followed the European Community Directive (86/609/EEC) and national rules on animal care that was carried out in accordance with the NIH Guidelines for the Care and Use of Laboratory Animals 8th edition.

Experimental protocol

Venom was milked from adult snakes collected from the western Nile delta in Egypt, in September, dried and reconstituted in saline solution prior to use. LD_{50} of venom was determined as described by Meier and Theakston (1986). To study the effect LD_{50} of the venom in kidney of rats after 4 h, rats were divided into two groups, six rats of each. Group I served as a control and received saline (0.2 ml saline/ rat) by intraperitoneal (*i.p.*) injection. Group II was injected *i.p.* with LD_{50} dose of *N. haje* venom in saline (0.025mg/kg). The animals of the two groups were sacrificed, and blood samples were collected by cardiac puncture. The blood stranded for half an hour and then centrifuged at 3,000 g for 15 min at 4ºC to separate serum and stored at -70ºC until analysis. The left kidney was weighed and homogenized immediately to give a 50% (w/v) homogenate in ice-cold medium containing 50 mM Tris-HCl, pH 7.4. The homogenate was centrifuged at 3,000 g for 10 min at 4ºC. The supernatant (10%) was used for the various biochemical determinations. Right kidney was cut into small pieces and kept for the histological and molecular studies.

Biochemical estimations

Kidney function test

Serum uric acid, urea and creatinine contents were determined colorimetrically by commercially available diagnostic kits (Biodiagonstic-Egypt) as per manufacturer's instructions.

Oxidative stress markers

Lipid peroxidation (LPO) in kidney was determined by using 1 ml of trichloroacetic acid 10% and 1 ml of thiobarbituric acid 0.67% and were then heated in a boiling water bath for 30 min. TBARS were determined by the absorbance at 535 nm and expressed as malondialdehyde (MDA) formed (Ohkawa *et al*., 1979). Also, nitric oxide was determined in acid medium and in the presence of nitrite the formed nitrous acid diazotized sulfanilamide is coupled with N-(1–naphthyl) ethylenediamine. The resulting azo dye has a bright reddish-purple color that can be measured at 540 nm (Green *et al*., 1982).

In addition, the renal glutathione (GSH) was determined by the reduction of Elman's reagent (5,5` dithiobis (2-nitrobenzoic acid) DTNB) with GSH to produce a yellow compound . The reduced chromogen directly proportional to GSH concentration and its absorbance can be measured at 405 nm (Ellman, 1959).

Enzymatic antioxidant status

The homogenates of kidney were used to determine the activities of superoxide dismutase (SOD) (Nishikimi *et al*., 1972), catalase (CAT) (Aebi, 1984), glutathione peroxidase (GPx) (Paglia and Valentine, 1967), glutathione-S-transferease (Habig *et al*., 1974) and glutathione reductase (GR) (Factor *et al*., 1998).

Flow cytometry

Pieces of kidney were prepared by manual disaggregation procedure. Briefly, a few drops of RPMI were added to tissue and then minced until complete tissue disaggregation was achieved. Suspended cells were filtered using a 50 µm pore size mesh and then centrifuged at 1000 g for 10 min. Cells were resuspended in phosphate buffer, counted and washed by calcium buffer then centrifuged at 1500 g for 5 min. The pellet was resuspended and then cells were counted. Annexin-PI apoptotic assay was carried out using IQP-120F Kit (IQ Products, Groningen, Netherlands). FAC scan Becton-Dickinson (BD) flow-cytometer was used and data were analyzed using cell Quest software.

Western blot analysis

Total proteins were extracted using RIPA buffer. Protein determination was applied by a Lowry method (Lowry *et al.*, 1951). Denatured proteins (20 µg) were size fractionated by 12.5% SDS-polyacrylamide gels. Proteins were transferred to nitrocellulose membrane at 30 V for 1 h. The blots were blocked for 1.5 h at room temperature in fresh blocking buffer (0.1% Tween-20 in Tris-buffered saline, pH7.4, containing 5% BSA). The membrane was incubated overnight at 4°C with primary antibodies against Bax, GPx, GR, SOD and mitochondrial respiratory complexes at dilution of 1:200. β-actin was used as a loading control. The membrane was incubated for 2 h with HRP-conjugated secondary antibodies at a dilution of 1:1000. Chemiluminescent signals were captured using an ECL-plus chemiluminescent kit (GE Healthcare, UK) and Kodak Luminescent Image Analyzer (Kodak In-Vivo Imaging Systems F).

Histopathology and p53 and caspase-3 immunohistochemistry

Small pieces of the kidney were quickly removed, then fixed in 10 % neutral buffered formalin. Following fixation, specimens were dehydrated, embedded in wax, and then sectioned to 5 microns thickness. For histological examinations, sections were stained with haematoxylin and eosin. Immunolocalization techniques for p53 and caspase-3 were performed on 3-4 µm thickness sections according to Pedrycz and Czerny (2008). For negative controls, the primary antibody was omitted. In brief, mouse anti-p53 or mouse anti-caspase-3 (diluted1:200, Santa Cruz Biotechnology, Santa Cruz, CA, USA), were incubated with sections for 60 min. Primary antibodies were diluted in Tris buffered saline (TBS)/1% BSA. Then a biotinylated secondary antibody directed against mouse immunoglobulin (Biotinylated Link Universal–DakoCytomation kit, supplied ready to use) was added and incubated for 15 min, followed by horse radish peroxidase conjugated with streptavidin (DakoCytomation kit, supplied ready to use) for a further 15 min incubation. At the sites of immunolocalization of the primary antibodies, a reddish to brown colour appeared after adding 3-amino-9-ethylcarbasole (AEC) (DakoCytomationkit, supplied ready to use) for 15 min. The specimens were counterstained with hematoxylin for 1min and mounted using the Aquatex fluid (Merck KGaA, Germany).

Scanning electron microscopic (SEM) study

Kidneys were removed, and cortical slices were cut into big pieces, which were immersed in Karnovsky's solution (2% glutaraldehyde, 2% paraformaldehyde in 0.1 M phosphate buffer, pH 7.4) at 4°C overnight. After rinsing in phosphate buffer for 1 h, the specimens were post-fixed in buffered 1% OsO_4 at 4°C in the dark for 2 h and then immersed in a 2.3 M sucrose solution at 4°C overnight. The specimens were subsequently immersed for 30 min in liquid nitrogen and then fractured, washed in the same buffer, dehydrated in a graded acetone series, and critical-point dried. After identifying the fractured surface, specimens were mounted on stubs, sputtered with gold for 120 s, and examined and photographed with a Zeiss DSM 940A SEM operated at 10 kV.

Transmission electron microscopic (TEM) study

Kidneys were removed, and cortical slices were cut into small pieces, which were immersed in the same fixative with 0.1% tannic acid and 5% sucrose for 3 h at room temperature. After rinsing in a sugar-saline solution (0.15 M NaCl, 0.2 M sucrose), the specimens were post-fixed with 1% OsO_4 at 4°C in the glucose-saline solution in the

dark for 2 h and then rinsed again in the glucose-saline solution. The samples were dehydrated in a graded ethanol series and embedded in Epon 812 resin at 60°C for 48 h. Thin sections (60–70 nm) were double-stained with uranyl acetate and lead citrate and were observed and photographed with a LEO 906 TEM operated at 60 kV.

Statistical analysis

The obtained data were presented as means ± standard deviation of the mean. Statistical analysis was performed using an unpaired Student's t-test using a statistical package program (SPSS version 17.0). Differences between groups were considered significant at $P<0.05$.

RESULTS

Kidney function parameters were affected by a single *i.p.* injection of Egyptian cobra (0.025 mg/kg). The levels of serum urea and creatinine were increased significantly (27.7 and 44.0%, respectively) in envenometed rats (Table I). However, the level of uric acid was significantly reduced (22.2%; $P<0.05$) after 4 h of venom injection compared to the control rats.

Table I.- Changes in kidney function of rats induced by Egyptian cobra venom after 4 h.

Parameters	Control rats	Intoxicated rats
Serum uric acid (mg/dL)	69.63±9.81	54.14±6.61*
Serum urea (mg/dL)	3.21±0.40	4.1±0.46*
Serum creatinine (mg/dL)	0.50±0.03	0.72±0.03*

Values are means ± SD (n=6). *: significant change at $P< 0.05$ with respect to the Control group.

Table II shows the potential oxidative stress effects of Egyptian cobra venom in the kidney homogenate. This was evidenced by the significant increase in the level of both of the lipid peroxidation and nitric oxide by 78.5 and 82.2%, respectively. The elevation in nitric oxide content of the kidney could be explained by up-regulation in iNOS gene that measured with RT-PCR (data not shown). Also, the glutathione level was significantly reduced by about 55% in the kidneys (Table II) of rats receiving the venom. Moreover, there was a reduction in GR, GST, and GPx by approximately, 28.6, 60.9 and 45.7%, respectively. Interestingly, the reduction in GR and GPx activities were accompanied by concomitant significant effect on its expression ($P<0.05$) (Fig. 1). The reduction in GR and GPx proteins expression were 24.1 and 15.1%, respectively. The reduction in GPx enzyme activity was also tested with RT-PCR method where GPx gene was down-regulated as compared with that of the control (data not shown).

Table II.- Changes in kidney oxidant/antioxidant state of rats induced by Egyptian cobra venom after 4 h.

Parameters	Control rats	Intoxicated rats
Tissue MDA (nmol/g tissue)	729.70±50.21	1302.82±81.66*
Tissue NO (µmol/g tissue)	100.94±7.73	183.89±13.10*
Tissue GSH (mmol/g tissue)	67.33±2.89	39.71±1.33*
Tissue GPx (U/g tissue)	2075.03±317.67	1125.77±203.39*
Tissue GR (µmol/h/g tissue)	140.67±22.01	100.48±23.62*
Tissue GST (µmol/h/g tissue)	0.23±0.06	0.09±0.01*
Tissue SOD (U/g tissue)	2.52±0.04	1.21±0.16*
Tissue CAT (U/g tissue)	1.51±0.16	0.96±0.12*

Values are means ± SD (n=6). *: significant change at $P< 0.05$ with respect to the Control group.

Severe inhibition of SOD and CAT activities (108.3 and 36.4%, respectively) were observed in the kidneys (Table II) of Egyptian cobra venom-injected rats compared to these of the controls. The inhibition in SOD was accompanied by a significant reduction in the expression of SOD after 4 h Egyptian cobra envenomation by approximately 49% ($P<0.05$).

Figure 1 shows alterations in the activities of mitochondrial respiratory complexes. Complex II, III and IV activities in the kidney tissue from envenomated rats were highly increased (40–100% from control; $P<0.05$). However, complex V showed a significant inhibition (32%; $P<0.05$) in its activity.

In the present investigation, the percentage of both of the apoptotic and necrotic cells in the kidney of Egyptian cobra venom-injected rats were 28.3 and 32.06%, respectively, up to the control (Fig. 2), while the viable cells were decreased down to -21.4% compared to the control samples.

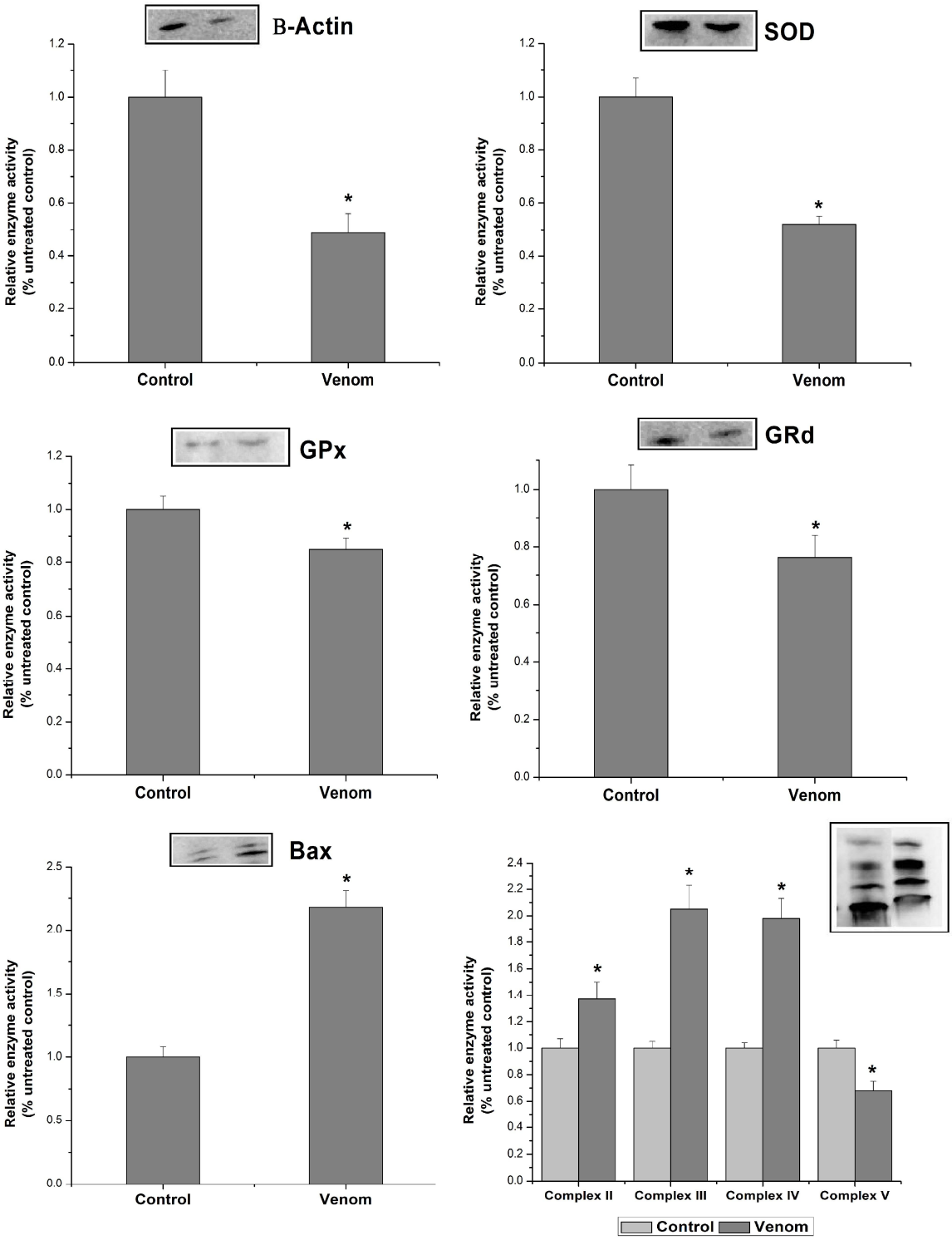

Fig. 1: Western blots showing the effects of Egyptian cobra venom on proteins expression of β–Actin, GPx, GR, SOD, Bax and complexes II, III, IV and complex V in the kidney after envenomation for 4 h.
Values are means ± SD (n=6). *: significant change at $P< 0.05$ with respect to the Control group.

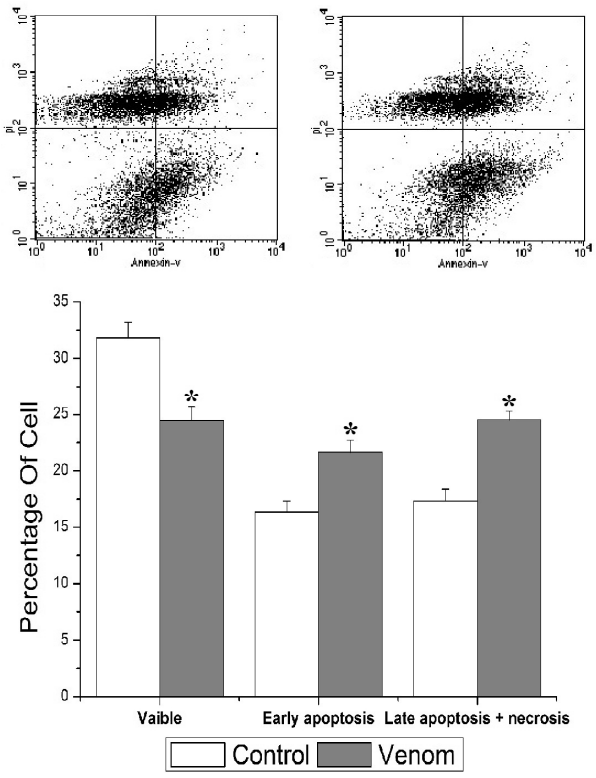

Fig. 2: Changes in viable, early apoptotic and late apoptotic and necrotic cells of kidney cells of rats induced by Egyptian cobra venom after 4 h.
Values are means ± SD (n=6). *: significant change at $P< 0.05$ with respect to the Control group.

Microscopic examination of the renal tissue shows that the venom induced a severe glomerular degeneration and coagulative necrosis. Also, the urinary spaces appeared wider as compared with the control one. Moreover, most of the renal tubules were degenerated and filed with cellular debris (Fig. 3B). Immunohistochemical findings in control kidneys showed a week immunoreactivity of both of caspase-3 and p53 (Fig. 3C,E, respectively) while, a strong positive reaction was detected in the sections of the venom injected group (Fig. 3D and F, respectively).

The ultrastructure of the glomeruli of the control animals showed capillary loops which embodied blood cells and precipitated plasma proteins. The capillaries are lined with a thin layer of flattened and fenestrated endothelial cells. The nuclei of such cells can be seen bulging into the capillary lumina. Mesangial cells and mesangial substance provides support for the capillary loops. The podocytes form the outer layer of the capillary wall, each has a cell body from which arise several primary processes. Each primary process gives rise to numerous secondary processes called pedicels that embrace the glomerulus capillaries. The fenestrated capillary endothelium is closely applied to the glomerular basement membrane and on the opposite side of the basement membrane are the podocytes secondary processes (pedicels) separated from each other by slight pores of approximately uniform width (Fig. 4A). The electron micrographs of the convoluted tubules of control animals reveal profuse, tall microvilli which represent the brush border seen with light microscopy. The plasma membrane at the bases of the cells of the tubules exhibits deep basal infoldings into the cells. These infoldings set up basal compartments that embody elongated mitochondria (Fig. 4B).

In the venom injected group, the glomeruli appeared with proliferated mesangial cells and most of the foot processes of the epithelial cells were discrete but few of these processes were fused together (Fig. 4C). On the other hand, the convoluted tubule showed deformity of the nuclei, mitochondria and the enfolding of the basement membrane. Extensive degenerative changes represented by lysis of many cell contents were notice (Fig. 4D).

SEM examination of the glomeruli tufts of normal rats showed many erythrocytes with various shapes, in the capillary networks and interdigitating foot processes (Fig. 5A). The convoluted tubules of normal rats contained basement membranes, mitochondria, nuclei infoldings and lamina (Fig. 5B). On the other hand, glomeruli of the venom injected rats were enlarged due to loss of mesangial cells and matrix. Also, the glomeruli appeared with a segmental ballooning lesion with honeycomb-like appearance on the surface (Fig. 5C). In addition, the convoluted tubules were damaged (Fig. 5D).

DISCUSSION

Several works dealing with the effects of snake venoms in blood cells, marrow cells and in cells from other organs of animals, like muscle, liver, kidney and skin, showed varying results, depending on the experimental concentrations,

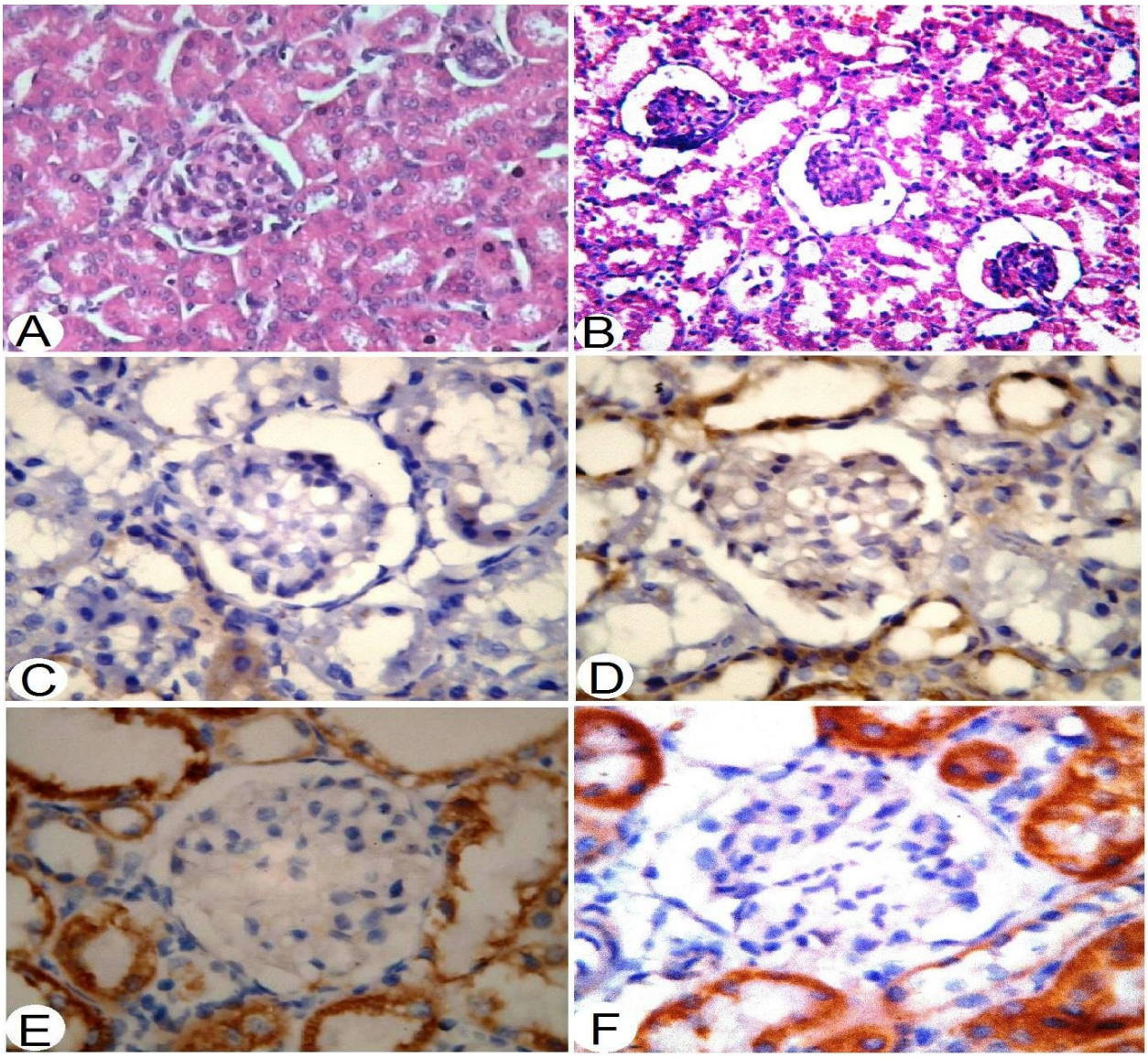

Fig. 3. Histological structure of kidney of A) Control rat show intact architecture of the glomerulus and renal tubules, B) Egyptian cobra venom injected rats with severe glomerular degeneration, wide urinary space, and degenerative renal tubules (H&E X 150), C) control rat appearing with no immunoreaction of caspase-3 in the cortical regions, D) Egyptian cobra venom injected rat shows strongly caspase-3 expression in inner cortical and outer medullary areas especially in the proximal convoluted tubules, whereas there is less caspase-3 expression in the glomerular structure (caspase-3 immunostaining X 300), E) control rat shows weak immunoreactivity of p53, and F) Egyptian cobra venom treated rat shows strong immunoreactivity of p53 (p53 immunostaining X 300).

exposure time, site of injection, and type of toxin (Maria *et al*., 2003; Fox and Serrano, 2008; Tohamy *et al*., 2014). In the present investigation, we explored the systemic physio-pathological changes induced by the Egyptian cobra venom in kidney as a vital organ. The high levels of creatinine and urea indicate an impairment of renal function. Similar observations were reported in rats following administration of various snake venoms (Omran and Abdel-Nabi, 1997; Schneemann *et al*., 2004). Such increased vascular permeability, together with renal damage would further aggravate the accompanying

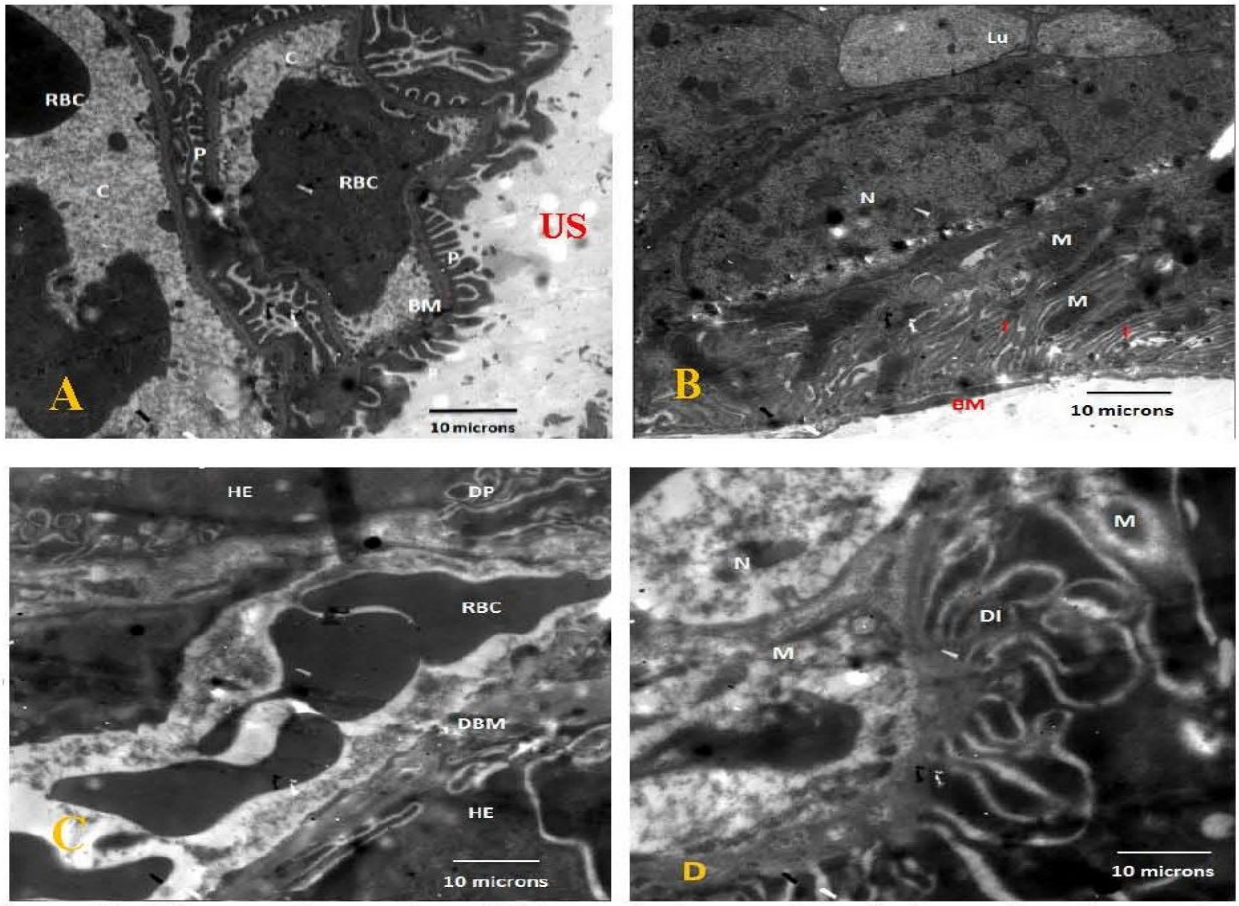

Fig. 4: Electronmicrographs of kidney of A) a portion of glomerulus of control rat shows two capillary loops (C). Notice the erythrocyte (RBC). The capillaries lined with thin fenestrated endothelial cells (EC). The primary podocyte processes (P1) give rise to numerous secondary foot processes (P2) which rest on the basement membrane of the capillary (BM), B): a part of distal convoluted tubule of control rat shows the enfolding of the basal membrane (BM), a large number of mitochondria (Mi) and a few number of microvilli (Mv). Notice the wide lumen of such tubule (LU), C) a portion of glomerulus of rat showing shows proliferation of the mesangial cells. Most of the foot processes of the epithelial cells were discrete but few of these processes were fused together, D) a part of convoluted tubule shows deformity of the nucleus (N), mitochondria (M) and the enfolding of the basement membrane (DI). Notice extensive degenerative changes represented by lysis of many cell contents (TEM, Micron bar, 10 μm)

hypoproteinemia. Furthermore, the rise in serum urea and creatinine associated with the reduction of serum uric acid level observed, in the present study, supports the proposed impairment of renal function. Similar observations were reported following various viper envenomation of rats (Sant and Purandare, 1972; Omran and Abdel-Nabi, 1997). The proteolytic and phospholipase A_2 activities of Egyptian cobra venoms have important cytotoxic effects (Kerns *et al*., 1999; Rowan *et al*., 1991; Barrington *et al*., 1986; Stefansson *et al*., 1990) and could contribute to the nephrotoxicity seen in the current study.

The ultrastructural alterations induced by the snake venom in the trilaminar structure of the glomerular basement membrane (GBM) suggest the involvement of physicoelectrostatic barrier sites. Podocytes and endothelial cells retain heparin sulfate (Stow *et al*., 1985) in the lamina rara external and internal of the GBM, and the feet processes are coated with sialoproteins that contribute to the anionic charges of the filtration

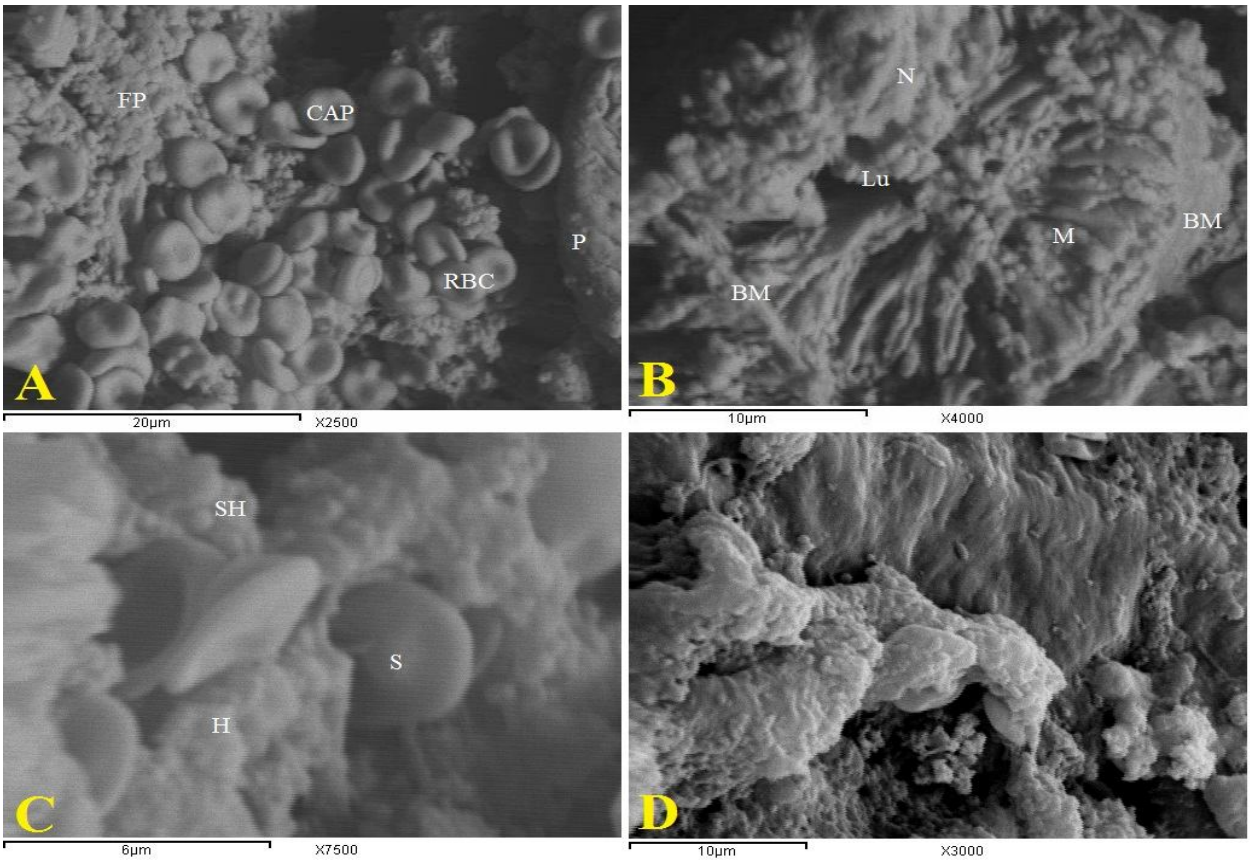

Fig. 5: Scanning Electron Microscopy micrographs of A): glomerular tufts of normal rats showing many erythrocytes (RBC) with various shapes, in the capillary (Cap) networks and interdigitating foot processes (FP) (Bar, 20 µm), B): convoluted tubule of normal rat showing basement membrane (BM), mitochondria (M), nucleus (N) infoldings (I) and lumen (Lu) (Bar, 10 µm), C): Glomerulus from venom treated rat showing capillaries are markedly distended and the glomerulus is enlarged due to loss of mesangial cells and matrix. Notice glomerulus shows segmental ballooning lesion with honeycomb-like appearance on the surface (H) (Bar, 8 µm), D) convoluted tubule from venom treated rat showing disturbance of the normal structure (Bar, 10 µm).

barrier (Kerjaschki *et al*., 1984). This ionic barrier of glomerular filtration was shown to be destroyed by *Vipera russelli* venom in isolated rat kidneys (Willinger *et al*., 1995). Furthermore, since the glomerular and renal tubule epithelial cells are strategically interposed between the extra and intramilieu, they are potential targets for numerous nephrotoxic agents, and the glomeruli are the first structure of the nephron to come in contact with circulating venom.

Snakebites are most often accompanied by signs of inflammation and local tissue damage (Nelson, 1989). Neutrophils and macrophages are induced to produce superoxide radical anion which belongs to a group of reactive oxygen species (ROS) and this reacts with cellular lipids leading to the formation of lipid peroxides and the observed necrosis (Valko *et al*., 2007). As the origin of oxidative stress is the mitochondrial respiratory electron transport chains (Fletcher *et al*., 1991), it is possible that mitochondrial death mediates venom-induced cellular damage (Haffor and Al-Sadoon, 2008; Abdel Moneim *et al*., 2014a).

It is generally accepted that a marked increase in Ca^{2+} could lead to ROS production. In many models of cell death it has also been proposed that ROS production is an early event in the process of apoptotic cell death. Furthermore, it had been proposed that ROS can also modulate gene expression by acting on transcription factors in a

variety of families like NF-κB, activator protein 1 (AP-1) and AP-2 (Ray *et al*., 2012). Also, *N. haje* venom contains cardiotoxins (CTX), a group of highly basic polypeptides of approximately 60 amino acids present in the many snakes, have ability to increase H_2O_2 production. All of these findings suggested that the renal cytotoxic effects of venom were apparently triggered by oxidative stress mediated by H_2O_2 and superoxide anion production. Generation of H_2O_2 in the mitochondria may result in mitochondrial peroxidation (Al-Quraishy *et al*., 2014).

Superoxide dismutase and catalase are considered as the primary antioxidant enzymes, since they are involved in the direct elimination of active oxygen species (Abdel Moneim *et al*., 2014b). Dai *et al*. (2012) have reported that, *Naja* sp. venoms have the SOD activity. Apart from this, in the past few years several peptides have been reported to exert deferent mechanisms of action in free radical mediated oxidative sequences by radical scavenging and metal ion chelation (Sri Balasubashini *et al*., 2006; Tohamy *et al*., 2014).

Many L-amino acid oxidase demonstrate apoptosis-inducing activity (Zhang and Wu, 2008) and it is partially due to the generation of hydrogen peroxide. Hydrogen peroxide belongs to ROS and it is widely accepted that mitochondrial perturbation has been associated with the increased production of ROS (Othman *et al*., 2014).

Expression of p53 as proapoptotic protein was significantly activated by Egyptian cobra venom. Moreover, our results showed that caspase-3 was most potently activated by the venom. Moreover, the present data suggest that the activation of caspase-3 is critical in snake venom-induced kidney damage. Also, p53 plays multiple roles in cell cycle control, differentiation, genomic stability, angiogenesis, and apoptosis (Maxwell and Davis, 2000). Miao *et al*. (1999) showed that the mRNA of p53 increased within 3 and 6 h after vascular endothelial cells were treated with rattle snake venom. Our results indicated that p53 plays an important role in apoptosis induced by Egyptian cobra venom in the kidney and they are in the same pathway in apoptotic signal transduction in the kidney.

CONCLUSIONS

The data presented herein suggested several aspects of the mechanisms of Egyptian cobra venom-induced renal toxicity. We proposed that: (i) Egyptian cobra venom induced apoptosis in kidney via activation of caspase-3 and modulation of the protein levels of Bax and Bcl-2; (ii) Egyptian cobra venom-activated p53 induced apoptosis; (iii) oxidative stress involved in transmitting apoptotic signals in Egyptian cobra venom-treated rats. These results provide valuable insight into the toxicity of Egyptian cobra venom and deepen our previous understanding of its molecular mechanisms of action.

Conflict of interests statement

The authors declare that there is no conflict of interests regarding the publication of this article.

ACKNOWLEDGEMENTS

The authors would like to extend their sincere appreciations to the Deanship of Scientific Research at King Saud University for its funding this Research group NO. (RG -1435-198).

REFERENCES

ABDEL MONEIM, A. E., ORTIZ, F., LEONARDO-MENDOCA, R. C., VERGANO-VILLODRES, R., GUERRERO-MARTÍNEZ, J. A., LÓPEZ, L. C., ACUÑA-CASTROVIEJO, D. AND ESCAMES, G., 2014a. Protective effects of melatonin against oxidative damage induced by LD_{50} *Naja haja* crude venom in rats. *Acta Trop.*, in press.

ABDEL MONEIM, A. E., OTHMAN, M. S. AND AREF, A. M., 2014b. *Azadirachta indica* attenuates cisplatin-induced nephrotoxicity and oxidative stress. *BioMed Res. Int.*, **11**: 647131.

AEBI, H., 1984. Catalase *in vitro. Methods Enzymol.*, **105**: 121-126.

AL-QURAISHY, S., DKHIL, M. AND ABDEL MONEIM, A. E., 2014. Hepatotoxicity and oxidative stress induced by *Naja haje* crude venom. *J. Venom. Anim. Toxins Incl. Trop. Dis.*, **20**: 42. doi:10.1186/1678-9199-20-42.

AL-SADOON, M. K., ORABI, G. M. AND BADR, G. 2013. Toxic effects of crude venom of a desert cobra, *Walterinnesia aegyptia*, on liver, abdominal muscles and brain of male albino rats. *Pakistan J. Zool*., **45**: 1359-1366

BARRINGTON, P. L., SOONS, K. R. AND ROSENBERG, P., 1986. Cardiotoxicity of *Naja nigricollis* phospholipase A2 is not due to alterations in prostaglandin synthesis. *Toxicon,* **24**: 1107-1116.

CHAIM-MATYAS, A., BORKOW, G. AND OVADIA, M., 1995. Synergism between cytotoxin P4 from the snake venom of *Naja nigricollis nigricollis* and various phospholipases. *Comp. Biochem. Physiol. B Biochem. Mol. Biol.,* **110**: 83-89.

DAI, G. L., HE, J. K., XIE, Y., HAN, R., QIN, Z. H. AND ZHU, L.J., 2012. Therapeutic potential of *Naja naja atra* venom in a rat model of diabetic nephropathy. *Biomed. Environ. Sci.,* **25**: 630-638.

EL HAKIM, A. E., GAMAL-ELDEEN, A. M., SHAHEIN, Y.E., MANSOUR, N.M., WAHBY, A.F. AND ABOUELELLA, A.M., 2011. Purification and characterization of a cytotoxic neurotoxin-like protein from *Naja haje haje* venom that induces mitochondrial apoptosis pathway. *Arch. Toxicol.,* **85**: 941-952.

ELLMAN, G.L., 1959. Tissue sulfhydryl groups. *Arch. Biochem. Biophys.,* **82**: 70-77.

FACTOR, V. M., KISS, A., WOITACH, J. T., WIRTH, P.J. AND THORGEIRSSON, S.S., 1998. Disruption of redox homeostasis in the transforming growth factor-alpha/c-myc transgenic mouse model of accelerated hepatocarcinogenesis. *J. biol. Chem.,* **273**: 15846-15853.

FLETCHER, J.E., JIANG, M.S., GONG, Q.H., YUDKOWSKY, M.L. AND WIELAND, S.J., 1991. Effects of a cardiotoxin from *Naja naja kaouthia* venom on skeletal muscle: involvement of calcium-induced calcium release, sodium ion currents and phospholipases A2 and C. *Toxicon,* **29**: 1489-1500.

FOX, J.W. AND SERRANO, S. M., 2008. Exploring snake venom proteomes: multifaceted analyses for complex toxin mixtures. *Proteomics,* **8**: 909-920.

GREEN, L.C., WAGNER, D.A., GLOGOWSKI, J., SKIPPER, P.L., WISHNOK, J.S. AND TANNENBAUM, S.R., 1982. Analysis of nitrate, nitrite, and [^{15}N]nitrate in biological fluids. *Anal. Biochem.,* **126**: 131-138.

GUTIERREZ, J. M., THEAKSTON, R. D. AND WARRELL, D.A., 2006. Confronting the neglected problem of snake bite envenoming: the need for a global partnership. *PLoS Med.,* **3**: e150.

HABIG, W. H., PABST, M. J. AND JAKOBY, W. B., 1974. Glutathione S-transferases. The first enzymatic step in mercapturic acid formation. *J. biol. Chem.,* **249**: 7130-7139.

HAFFOR, A.S. AND AL-SADOON, M.K., 2008. Increased antioxidant potential and decreased free radical production in response to mild injection of crude venom, *Cerastes cerastes gasperetti*. *Toxicol. Mech. Methods,* **18**: 11-16.

JOUBERT, F. J. AND TALJAARD, N., 1978. *Naja haje haje* (Egyptian cobra) Venom. *Eur. J.Biochem.,* **90**: 359-367.

KERJASCHKI, D., SHARKEY, D. J. AND FARQUHAR, M.G., 1984. Identification and characterization of podocalyxin--the major sialoprotein of the renal glomerular epithelial cell. *J. Cell Biol.,* **98**: 1591-1596.

KERNS, R. T., KINI, R. M., STEFANSSON, S. AND EVANS, H.J., 1999. Targeting of venom phospholipases: The strongly anticoagulant phospholipase A2 from *Naja nigricollis* venom binds to coagulation factor Xa to inhibit the prothrombinase complex. *Arch. Biochem. Biophys.,* **369**: 107-113.

LOWRY, O. H., ROSEBROUGH, N. J., FARR, A.L. AND RANDALL, R.J., 1951. Protein measurement with the Folin phenol reagent. *J. biol. Chem.,* **193**: 265-275.

MARIA, D.A., VASSAO, R.C. AND RUIZ, I.R., 2003. Haematopoietic effects induced in mice by the snake venom toxin jararhagin. *Toxicon,* **42**: 579-585.

MARKLAND, F.S., 1998. Snake venoms and the hemostatic system. *Toxicon,* **36**: 1749-1800.

MAXWELL, S.A. AND DAVIS, G.E., 2000. Differential gene expression in p53-mediated apoptosis-resistant vs. apoptosis-sensitive tumor cell lines. *Proc. natl. Acad. Sci. USA,* **97:** 13009-13014.

MEIER, J. AND THEAKSTON, R.D., 1986. Approximate LD_{50} determinations of snake venoms using eight to ten experimental animals. *Toxicon,* **24**: 395-401.

MIAO, J.Y., ARAKI, S., HAN, Y.R. AND HAYASHI, H., 1999. Involvement of gene expressions in apoptosis of vascular endothelial cells induced by rattlesnake venom. *Cell Res.,* **9**: 237-242.

MUKHERJEE, A. K., GHOSAL, S. K. AND MAITY, C., 1998. Effect of oral supplementation of vitamin E on the hemolysis and erythrocyte phospholipid-splitting action of cobra and viper venoms. *Toxicon,* **36**: 657-664.

MUKHERJEE, A.K. AND MAITY, C.R., 1998. The composition of *Naja naja* venom samples from three districts of West Bengal, India. *Comp. Biochem. Physiol. A Mol. Integr. Physiol.,* **119**: 621-627.

NELSON, B.K., 1989. Snake envenomation. Incidence, clinical presentation and management. *Med. Toxicol. Adv. Drug Exp.,* **4**: 17-31.

NISHIKIMI, M., APPAJI, N. AND YAGI, K., 1972. The occurrence of superoxide anion in the reaction of reduced phenazine methosulfate and molecular oxygen. *Biochem. biophys. Res. Commun.,* **46**: 849-854.

OHKAWA, H., OHISHI, N. AND YAGI, K., 1979. Assay for lipid peroxides in animal tissues by thiobarbituric acid reaction. *Anal. Biochem.,* **95**: 351-358.

OMRAN, M. A. AND ABDEL-NABI, I.M., 1997. Changes in the arterial blood pressure, heart rate and normal ECG parameters of rat after envenomation with Egyptian cobra (*Naja haje*) venom. *Hum. exp. Toxicol.,* **16**: 327-333.

OTHMAN, M. S., SAFWAT, G., ABOULKHAIR, M. AND ABDEL MONEIM, A.E., 2014. The potential effect of

berberine in mercury-induced hepatorenal toxicity in albino rats. *Fd. Chem. Toxicol.,* **69**: 175-181.

PAGLIA, D. E. AND VALENTINE, W.N., 1967. Studies on the quantitative and qualitative characterization of erythrocyte glutathione peroxidase. *J. Lab. clin. Med.*, **70**: 158-169.

PEDRYCZ, A. AND CZERNY, K., 2008. Immunohistochemical study of proteins linked to apoptosis in rat fetal kidney cells following prepregnancy adriamycin administration in the mother. *Acta Histochem.,* **110**: 519-523.

RAHMY, T.R., 2001. Action of cobra venom on the renal cortical tissues: electron microscopic studies. *J. Venom. Anim. Toxins,* **7**: 85-112.

RAY, P. D., HUANG, B. W. AND TSUJI, Y., 2012. Reactive oxygen species (ROS) homeostasis and redox regulation in cellular signaling. *Cell Signal,* **24**: 981-990.

ROWAN, E.G., HARVEY, A.L. AND MENEZ, A., 1991. Neuromuscular effects of nigexine, a basic phospholipase A2 from *Naja nigricollis* venom. *Toxicon,* **29**: 371-374.

SANT, S. M. AND PURANDARE, N. M., 1972. Autopsy study of cases of snake bite with special reference to the renal lesions. *J. Postgrad. Med.,* **18**: 181-188.

SCHNEEMANN, M., CATHOMAS, R., LAIDLAW, S. T., EL NAHAS, A. M., THEAKSTON, R. D. AND WARRELL, D. A., 2004. Life-threatening envenoming by the Saharan horned viper (*Cerastes cerastes*) causing micro-angiopathic haemolysis, coagulopathy and acute renal failure: clinical cases and review. *Quart J. Med.,* **97**: 717-727.

SRI BALASUBASHINI, M., KARTHIGAYAN, S., SOMASUNDARAM, S. T., BALASUBRAMANIAN, T., VISWANATHAN, V., RAVEENDRAN, P. AND MENON, V.P., 2006. Fish venom (*Pterios volitans*) peptide reduces tumor burden and ameliorates oxidative stress in Ehrlich's ascites carcinoma xenografted mice. *Bioorganic. Med. Chem. Lett.,* **16**: 6219-6225.

STEFANSSON, S., KINI, R. M. AND EVANS, H. J., 1990. The basic phospholipase A2 from *Naja nigricollis* venom inhibits the prothrombinase complex by a novel nonenzymatic mechanism. *Biochemistry,* **29**: 7742-7746.

STOW, J. L., SAWADA, H. AND FARQUHAR, M.G., 1985. Basement membrane heparan sulfate proteoglycans are concentrated in the laminae rarae and in podocytes of the rat renal glomerulus. *Proc. natl. Acad.Sci. USA,* **82**: 3296-3300.

TOHAMY, A. A., MOHAMED, A. F., ABDEL MONEIM, A. E. AND DIAB, M. S. M., 2014. Biological effects of *Naja haje* crude venom on the hepatic and renal tissues of mice. *J. King Saud Univ. Sci.,* **26**: 205-212.

VALKO, M., LEIBFRITZ, D., MONCOL, J., CRONIN, M. T., MAZUR, M. AND TELSER, J., 2007. Free radicals and antioxidants in normal physiological functions and human disease. *Int. J. Biochem. Cell. Biol.,* **39**: 44-84.

WILLINGER, C. C., THAMAREE, S., SCHRAMEK, H., GSTRAUNTHALER, G. AND PFALLER, W., 1995. In vitro nephrotoxicity of Russell's viper venom. *Kidney Int.,* **47**: 518-528.

ZHANG, L. AND WU, W.T., 2008. Isolation and characterization of ACTX-6: a cytotoxic L-amino acid oxidase from *Agkistrodon acutus* snake venom. *Nat. Prod. Res.,* **22**: 554-563.

(Received 16 August 2014, revised 16 September 2014)